Dynamics of Grain Avalanches

Jean Rajchenbach

Laboratoire des Milieux Désordonnés et Hétérogènes (CNRS-UMR 7603)–Case 86, Université Pierre et Marie Curie, 4 Place Jussieu, 75252 Paris Cedex 05, France

(Received 17 July 2001; published 14 December 2001)

We study the nucleation and the growth of avalanches in a model experimental system consisting of a bidimensional packing of noncohesive grains positioned in a rotating drum. We show that the avalanche mass increases linearly in time, and that the growth rate is governed by the velocities of the two up and down fronts. The upper front is shown to propagate upwards with a velocity which is equal to the averaged velocity of the flowing grains, whereas the velocity of the downslope propagating front is approximately equal to twice the avalanche velocity. We describe simple mechanisms which quantitatively account for the observed dynamical properties.

DOI: 10.1103/PhysRevLett.88.014301 PACS numbers: 45.70.Ht, 05.65.+b, 47.50.+d, 83.80.Fg

The control of particulate flows is most important both for improvements of industrial processes and for the prevention of natural disasters, such as avalanches or landslides [1,2]. Understanding the physical mechanisms leading to triggering and growth of avalanches is thus of major interest. We focus here on the avalanche properties of a model system of noncohesive grains. Such model systems were previously shown to manifest different types of flows, according to the magnitude of the supply flux [3]. For a large flux, the flow appears to be continuous, in opposition to the regime of weak supply flux for which the flow displays a series of discrete avalanches. The existence of these two different regimes originates in the requirement for the free surface slope to overpass a certain angle θ_{start} to initiate the flow. If the spontaneous discharge rate of the surface flow is not balanced by the uphill supply flux, the slope progressively decreases and the flow stops (at angle θ_{stop}). Then a new avalanche is generated after the delay time required to store enough matter and to increase again the slope up to the angle θ_{start}. On the contrary, if the supply flux is larger than the natural discharge rate of one avalanche, the continuous flow regime is encountered.

Such description of the discrete avalanche process enters the scheme of the ubiquitous "relaxation oscillations." Several authors developed an analogy with the stick-slip motion of a block relying on a frictional substrate and bound to a spring pulled with a constant velocity [4]. In solid friction, the stick-slip behavior proceeds from the difference of magnitude between the "static coefficient of friction" μ_{stat} and the "dynamic coefficient of friction" μ_{dyn} ($\mu_{\text{stat}} > \mu_{\text{dyn}}$). Within this analogy, the elastic energy stored in the spring corresponds to the gravity potential energy of the heap, and the intermittent block velocity to the flux. From the relation between Coulomb's friction coefficient of the bulk material and the free surface slope, $\tan\theta_{\text{start}}$ can be identified with μ_{stat} and $\tan\theta_{\text{stop}}$ with $(2\mu_{\text{dyn}} - \mu_{\text{stat}})$.

Another interesting approach is that of Bouchaud, Cates, Ravi-Prakash, and Edwards (BCRE), who considered the grain avalanche as a multiplicative process [5]. They considered two coupled variables, the thickness h of the immobile substrate and the thickness R of the flowing layer (both expressed in grain-diameter unit). The boundary between the flowing layer and the substrate at rest can move, owing to erosion or accretion processes. Bouchaud *et al.* proposed to describe the erosion or accretion term depending linearly on the deviation $(\theta - \theta_{\text{stop}})$ from the static angle of repose θ_{stop}. The destabilization (or redeposition) efficiency is assumed further to be proportional to the number of flowing particles, and the mass conservation can hence simply be expressed as a dynamical equation for the number of immobile grains $h(x,t)$ [whose derivative $\partial h(x,t)/\partial x$ determines the local substrate slope]: $\partial h(x,t)/\partial t = -\gamma R(x,t)(\theta - \theta_{\text{stop}})$. Here γ is the collision rate [$\gamma \approx (g/d)^{1/2}$, where g is the gravity constant and d is the grain diameter]. Next, Bouchaud *et al.* approximate that the grain fall velocity $\overline{v}$ is a constant throughout the whole flowing layer. They obtain therefore, for the local dynamics of the rolling grains, $\partial R(x,t)/\partial t = \gamma R(x,t)(\theta - \theta_{\text{stop}}) + \overline{v}\partial R(x,t)/\partial x + D\partial^2 R(x,t)/\partial x^2$. The first term on the right-hand side corresponds to the erosion/accretion processes, the second term describes the advective displacement of the flowing grains, and the last, diffusive term corresponds to the avalanche spreading. The magnitude of $\overline{v}$ is given by the limiting velocity between two collisions: $\overline{v} \approx (gd)^{1/2}$. If one considers now the development of a packet of rolling species located at $x = 0$ at time $t = 0$ in the case $\theta > \theta_{\text{stop}}$, the packet is convected downhill with a velocity $\overline{v}$, is amplified as $\exp[\gamma(\theta - \theta_{\text{stop}})t]$, and spreads as $(4Dt)^{1/2}$ (the slope variation due to erosion is neglected). Hence, the number of rolling grains located at $x = 0$ varies in time as $R(0,t) = (4\pi Dt)^{-1/2}\exp[\gamma(\theta - \theta_{\text{stop}})t - (v^2 t/4D)]$. Within this approach, the convection-diffusion mechanism is thus shown to shift the limiting slope which separates the avalanche amplification from the damping regime. For $\theta > \theta_{\text{stop}} + v^2/4D\gamma$ rolling grains are generated faster than they are convected downwards, and this leads to an

 0031-9007/02/88(1)/014301(4)$15.00 © 2001 The American Physical Society

exponential increase of the avalanche mass. On the other hand, for $\theta < \theta_{\text{stop}} + v^2/4D\gamma$, avalanches shrink.

In this paper we investigate the nucleation and amplification processes of avalanches, in a bidimensional model system. We show that the growth rate of the avalanches is determined by the difference of the velocities of the two (uphill and downhill) propagating fronts. The two front velocities are determined experimentally, and microscopic mechanisms are then proposed, which simply account for the observed dynamical properties.

The experimental setup has been described with further details elsewhere (see Refs. [3,6,7]). It mainly consists of a hollow aluminum cylinder (20-cm diameter) rotating around its horizontal axis at a constant speed. The container is partly filled with grains. Experiments are conducted with a monodisperse collection of steel spheres (ball bearings, of diameter $d = 1.5$ mm), with Young's modulus $Y = 200$ GPa and friction coefficient $k \approx 0.1$. The elastic restitution coefficient of the particles is $e = 0.93$. The grains are confined between two vertical glass faces, separated by one bead diameter. Thus the packing is bidimensional, and the lateral glass walls allow a visualization of the internal pile structure and an access to the grain velocities, which are continuously recorded by means of a fast camera (250 frames/second) and associated computer image processing. The rotation speed of the drum is monitored at 0.1 rpm. For this rotation velocity, the flow displays a discrete regime of well separated avalanches, distributed in size roughly according to a Gaussian statistics [7]. Upper layers of particles intermittently flow on the substrate which experiences a slow solid-body rotational motion. The typical duration of one avalanche is 1 sec, and the delay type between two consecutive avalanches is of the order of 10 sec.

Figure 1 shows a series of snapshots showing the nucleation and the propagation of a typical avalanche. Several noticeable features can be pointed out. First, the most unstable particle (or block of particles) is first destabilized, due to continuous solid rotation of its supporting basis beneath it. Second, we observe the propagation of a kinematic wave uphill, which corresponds to the onset into motion of uphill adjacent particles leaning on the previously starting grains. At the same time, we observe that adjacent neighboring particles lying downstream undergo shocks from the downward granular jump, triggering their motion. So, the jump is permanently refreshed and formed of new grains just entering into motion. We will describe this effect with further details below.

It is important to determine whether the upstream and downstream propagating fronts experience an accelerated regime, or rapidly attain their limiting velocities, and what the phenomena are that drive these two velocities. Figure 2 shows the absolute value of the distance covered by these two fronts as a function of time. The experimental points have been averaged on 20 runs of avalanches growing up to the limit imposed by the setup boundaries. We cannot distinguish any accelerated transient regime within our experimental accuracy: the two sets of experimental points can be fitted to straight lines. We can also directly measure the thickness of the flowing layer through the lateral wall. We observe that the flowing layer quickly attains the steady regime thickness, which is of the order of 7–10 grain sizes. Since both upstream and downstream fronts propagate with constant velocities, we realize that the avalanching mass increases linearly in time in the two-dimensional geometry. In three dimensions, if the lateral velocity also attains a steady state regime, we expect this relation to generalize as mass $\propto$(time)^2. From the direct access to the individual grain dynamics, we can extract the average magnitude $\overline{v}$ of their velocity: we find $\overline{v} \approx 10$ cm/s, which compares well with $\sqrt{gd\sin\theta} = 9.2$ cm/s. We remark, moreover, that the magnitude of $\overline{v}$ coincides with that of the upward propagating kinematic wave. We can explain this interesting property by means of the following simple argument. There is a source term for the number of falling particles,

(a)

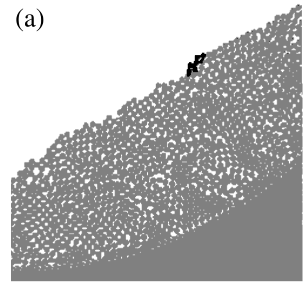

(b)

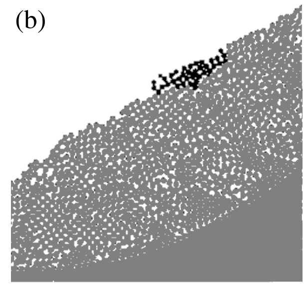

(c)

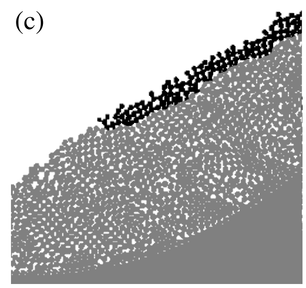

FIG. 1. Sequence of pictures showing the nucleation and the propagation of an avalanche. Here flowing grains are tagged in black and the delay time between each snapshot is 0.1 s. In (a), the most unstable particle (or block of particles) is first destabilized. In (b) and (c), we observe the propagation of a kinematic wave upslope, which corresponds to the onset into motion of uphill adjacent particles leaning on the previously starting grains. Simultaneously, adjacent neighboring particles lying downstream undergo shocks from the downward granular jump, triggering their motion. The velocity of the downhill propagating jump is twice ($\pm 10\%$) the depth-averaged velocity of the flowing layer.

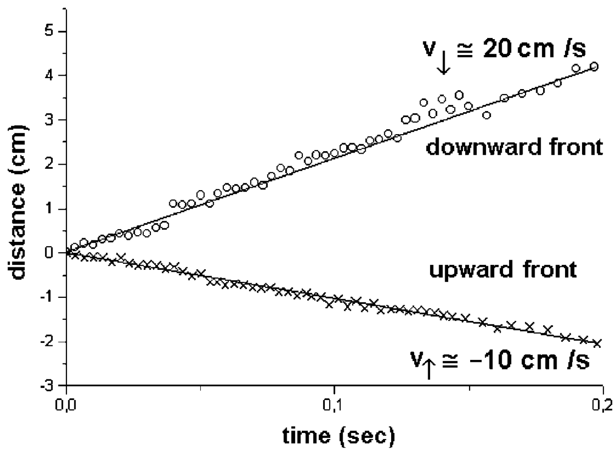

FIG. 2. Distances covered by the downwards and upwards propagating fronts as a function of time (averaged on 20 avalanche runs). In both cases, we are unable to detect any transient regime: the limiting velocity is reached very fast. The average velocity of the downhill propagating front is approximately $v_\downarrow \approx 20$ cm/s, while that of the uphill propagating front is $v_\uparrow \approx 10$ cm/s. This last one compares with the depth-averaged velocity $\overline{v}$ of the flowing layer.

which is related to the advance of the destabilizing front upslope. The number of new destabilized particles (per unit time) reads as $dN/dt = \nu_{\mathrm{stat}} v_\uparrow h'$, where ν_{stat} stands for the areal density of grains in the frozen phase and h' for the thickness of the front. On the other hand, the flow rate of grains is $dN/dt = \nu_{\mathrm{dyn}} \overline{v} h$, where ν_{dyn} is the areal density of the flowing phase and h is the thickness of the avalanche, which identifies with that of the front ($h = h'$). Since there is no major difference of densities between the immobile and flowing phases $[(\nu_{\mathrm{stat}} - \nu_{\mathrm{dyn}})/\nu_{\mathrm{dyn}} < 0.1]$, $v_\uparrow \approx \overline{v}$ ensues. Note that the BCRE model also leads to the existence of kinematic waves. Equating the exponential term to unity in $R(0, t)$ gives the typical velocities of the tails of the flowing bulge [8]. The velocity of the upper front is thus given by

$$v_\uparrow = -\frac{D\gamma}{v}(\theta - \theta_{\mathrm{start}}), \tag{1}$$

($\theta_{\mathrm{start}} = \theta_{\mathrm{stop}} + v^2/4D\gamma$) and can therefore propagate upwards or downwards according to whether $\theta > \theta_{\mathrm{start}}$ or $\theta < \theta_{\mathrm{start}}$. Within the BCRE model, the front velocity is precisely zero when $\theta = \theta_{\mathrm{start}}$ [8], while our measurement clearly shows that $|v_\uparrow| \approx |\overline{v}|$.

Another remarkable experimental feature that can be deduced from Fig. 2 is that the velocity of the downstream propagating front is approximately twice that of the upstream propagating front. Here it is important to point out that the properties of an avalanche falling on a noncohesive bed composed of grains of the same nature drastically depart from those occurring on a solid substrate that cannot be eroded. The last situation was, for instance, studied in experiments conducted in inclined channels, with rough bottoms [9,10]. In the case studied here, the downward front propagates faster than the depth-averaged velocity of the flowing layer. On the contrary, considerations on mass conservation lead to precisely identify the front velocity $v_\downarrow$ with the average avalanche velocity $\overline{v}$ in the case of nonerosive substrates.

In order to get a microscopic insight into the mechanism which governs the lower front velocity, we present in Fig. 3 the distance covered by the lower front as a function of time for a typical avalanche run. We recognize a steplike function, made up of inclined segments separated by quasivertical discontinuities. The slope of the segments is identical to the depth-averaged velocity $\overline{v}$ of the flowing layer, whereas the jumps correspond to sudden advances of the front downslope. Corresponding sets of pictures elucidate this phenomenology. Sudden discontinuities correspond to the destabilization of grain blocks as a whole, and their magnitude corresponds to block sizes. On the other hand, there is no destabilization of new grains downstream during the plateau events. Concerning the upper front, a detailed observation reveals that its upslope advance also occurs via collective destabilization of grain blocks. But there in contrast the front remains motionless between two successive destabilization events.

An explanation of the relation $v_\downarrow \approx 2\overline{v}$ can proceed from the statement that, at a microscopic level, the advance of the fronts is characterized by the intermittent destabilization of adjacent blocks downstream. For the sake of simplicity, consider first that the initial piling at rest displays a sinusoidal modulation of the free surface, with wavelength λ (Fig. 4). During the advance of the front over a depleted region downslope, no new grains are destabilized, and the velocity of the front coincides with the depth-averaged velocity $\overline{v}$ of the flowing layer. In contrast, when the front meets and collides with a bump at rest, this last one is (quasi)instantaneously destabilized as a whole, so that the front advances suddenly over a distance $\lambda/2$. Those intermittent events occur with frequency $1/\tau = 2\overline{v}/\lambda$. Hence we can write for the time averaged

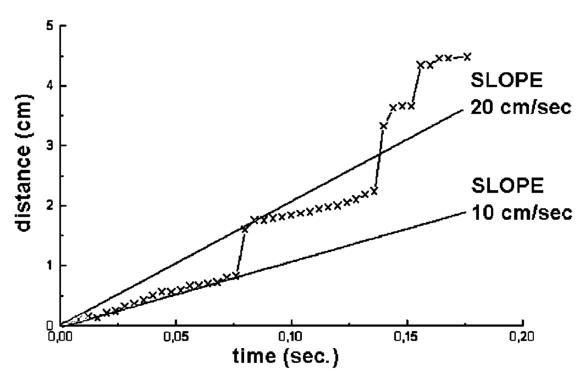

FIG. 3. A small-scale look at the advance of the downhill propagating front as a function of time (for one avalanche run). The quasivertical discontinuities correspond to sudden destabilization of blocks of particles adjacent to the downwards propagating front. The slope between two destabilization events corresponds to the depth-averaged avalanche velocity $\overline{v}$.

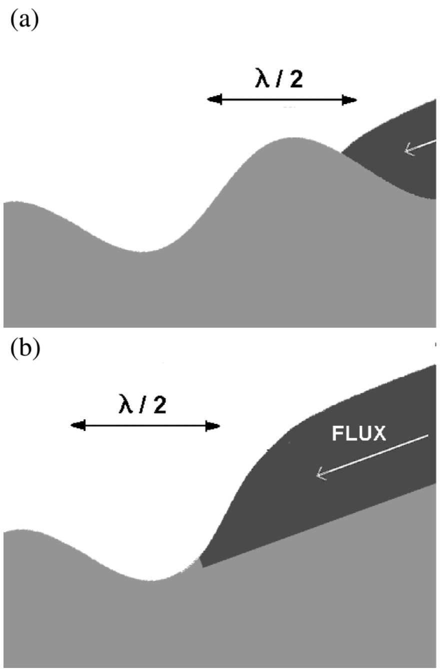

FIG. 4. Schematic model describing the downward front advance. Bumps are successively destabilized, owing to the shocks caused by the downslope propagating jump. This corresponds to sudden and discontinuous advances of the front. Between two destabilization events, the front advances with the average avalanche velocity $\overline{v}$ over a distance which compares with the average bump size $\lambda/2$. The delay time between two destabilization events reads hence $\tau = \lambda/2\overline{v}$. This schematic description allows one to explain the relation $v_\downarrow \approx 2\overline{v}$.

velocity of the downslope front

$$v_\downarrow = \overline{v} + \frac{\lambda}{2}\frac{1}{\tau} = 2\overline{v}\,. \qquad (2)$$

It is worth noting that relation (2) does not depend on the hypothesized initial wavelength λ and actually holds whatever the roughness of the free surface. It simply proceeds from the statement that the average distance separating two successive block destabilizations is identical with the mean block size. We also addressed the effect of the grain micromechanical properties (dry friction and elastic restitution coefficients) by performing measurements of $v_\downarrow$ and $v_\uparrow$ with more frictional, less elastic grains (Fontainebleau sand). In the case of more dissipative materials one might have expected a decrease of the down front destabilization efficiency and consequently a decrease of the ratio $R = v_\downarrow/v_\uparrow$. Surprisingly, the relation $R \approx 2$ seems to persist in the case of real sand. Moreover, the ratio R seems also not to depend on the setup dimensionality. Revisiting the snapshot reported in Fig. 4 of Ref. [11] shows that $R \approx 2$ is also obtained for glass beads in a 3D geometry. Nevertheless, we notice here some differences with the experiment performed by Daerr *et al.* [11]. These authors observed the upper boundary of the avalanche propagating downwards over a certain range of surface inclinations. But they also found an upwards propagating front for larger angles. We suggest that this difference originates in dissimilar experimental procedures. Daerr *et al.* chose to trigger the onset of avalanches by externally perturbing the free surface with a probe, thus providing the dilatancy required to start the grain moving by hand. In contrast, using here a rotating drum we observe avalanches whose nucleation occurs spontaneously, due to the progressive increase of the slope.

To conclude, we showed that the two-dimensional avalanching masses are mainly characterized by the velocities of the two up and down fronts, since the thickness rapidly reaches its steady value. We carried out experimental determinations of these two velocities, and found that the magnitude of the velocity of the upstream propagating front can be identified with the average velocity of the flowing grains, whereas the velocity of the downslope propagating front corresponds to twice the depth-averaged avalanche velocity. This feature does not seem to depend noticeably on the dissipative properties of the flowing material nor on the space dimensionality. On the other hand, we presented evidence that the front dynamics is mainly ruled by the erosive properties of the substrate. We also found that the 2D avalanche mass varied linearly in time, and we suggest a generalization as mass $\propto(\text{time})^2$ in 3D geometry. Finally we proposed a simple explanatory scheme qualitatively accounting for our experimental findings.

We acknowledge A. Daerr for interesting discussions and E. Bringuier for a critical reading of the manuscript.

[1] B. J. Ennis, in *Powders and Grains 97,* edited by R. P. Behringer and T. J. Jenkins (A. A. Balkema, Rotterdam, 1997), p. 13.
[2] K. Hutter, in *Hydrology of Disasters,* edited by V. P. Singh (Kluwer Academic Publishers, Dordrecht, 1996).
[3] J. Rajchenbach, Phys. Rev. Lett. **65**, 2221 (1990). For a recent review, see J. Rajchenbach, Adv. Phys. **49**, 229 (2000).
[4] C. Caponeri, S. Douady, S. Fauve, and S. Laroche, in *Mobile Particulate Systems,* edited by E. Guazzelli and L. Oger (Kluwer Academic Publishers, Dordrecht, 1995), p. 331; S. J. Linz and P. Hänggi, Phys. Rev. E **50**, 3464 (1994).
[5] J. P. Bouchaud, M. E. Cates, J. Ravi-Prakash, and S. F. Edwards, Phys. Rev. Lett. **74**, 1982 (1995); J. Phys. I (France) **4**, 1383 (1994).
[6] F. C. Franklin and L. N. Johanson, Chem. Eng. Sci. **4**, 119 (1935).
[7] P. Evesque and J. Rajchenbach, C. R. Acad. Sci. (Paris), Sér. 2 **307**, 223 (1988).
[8] J. P. Bouchaud and M. E. Cates, in *Physics of Dry Granular Media,* edited by H. J. Herrmann, J. P. Hovi, and S. Luding (Kluwer Academic Publishers, Dordrecht, 1998), p. 465.
[9] S. B. Savage and K. Hutter, J. Fluid Mech. **199**, 177 (1989).
[10] O. Pouliquen, Phys. Fluids **11**, 542 (1999).
[11] A. Daerr and S. Douady, Nature (London) **399**, 241 (1999); A. Daerr, thesis, Université Paris VII, 2000.